ALKALI-ACTIVATION OF RECYCLED CONCRETE WASTE

Edna Paula da Costa Reis[1], Guilherme Jorge Brigolini Silva[2] and
Jose Carlos Borba Jr[3].

[1]Post-Graduate Program of Construction Engineering, Federal University of Ouro Preto,
Ouro Preto, Brazil.
edna.paula@ufop.edu.br
[2]Department of Civil Engineering, Federal University of Ouro Preto, Ouro Preto, Brazil.
guilhermebrigolini@ufop.edu.br
[3]Department of Technology in Civil Engineering, Computation, Humanities and Automation,
Federal University of São João Del-Rey, Ouro Branco, Brazil.
joseborba@ufsj.edu.br

ABSTRACT

Civil construction is one of the sectors that most cause environmental impacts. Given this scenario, it is extremely important to develop new technologies that contribute to making civil construction a sector with less polluting potential. Stations the exploratory-research presentation of an alkali-activated material (AAM) with cementitious properties using the study of recycled concrete as a precursor. After concrete preparation by grinding and sieving, the material precursor was prepared by X-ray fluorescence, X-ray diffraction, laser diffraction granulometry and SEM-SE. Five different mixes in the production of different silicas and hydroxides of 3% and 9% of contents of 0%, 2% and 8% content. After curing 10°C as masses, they were from 0 to 7 days of curing tests X-ray diffraction and thermal resistance through tests. The highest bond strength was 14MPa. In the XRD assay there was no formation of new crystalline phases. The SEM/EDS analysis suggests a formation of a C-A-S-H gel. The material characterization assays for the possibility of using AAM.

KEYWORDS: civil construction, alkali-activated material, recycled concrete residue.

I. INTRODUCTION

Civil construction is a prominent contributor to environmental perturbation, stemming from diverse sources such as non-renewable resource extraction, energy consumption, greenhouse gas emissions, and copious solid waste generation [1]. Construction and Demolition Waste (CDW), currently representing the highest fraction of global waste production [2, 3], poses a significant environmental concern. In Brazil, for instance, CDW accounted for approximately 57% of urban solid waste in 2020, equivalent to an estimated 47 million tons [4]. This waste category is dominated by concrete and masonry, constituting around 31.3% of the total generated construction waste [5]. The sheer volume of CDW, coupled with improper disposal practices, intensifies environmental degradation [6].

Amid this backdrop, the imperative of fostering less ecologically intrusive practices within civil construction looms large. Utilizing waste materials in the creation of construction materials emerges as an ecologically sound solution for their management. Diverse by-products, industrial discards, and aluminosilicates have been harnessed to develop Alkali-Activated Materials (AAM) that supplant traditional Portland cement [7]. The wealth of available materials permits global repositories of discarded substances to be harnessed advantageously.

The process of producing AAM centers on alkaline activation—a chemical transformation enabling the conversion of certain partially or entirely amorphous structures into compact cementitious materials. This process hinges on the reaction of solid aluminosilicates (precursors) under alkaline conditions induced by an alkaline activator, yielding a solidified paste [8]. An analogous definition posited by

Severo et al. underscores alkaline activation as the hydration reaction of aluminosilicates catalyzed by alkaline and alkaline earth substances [9].

Scholarly attention has increasingly gravitated towards the prospect of alkaline activating waste residues, due to its potential to yield cost-effective and environmentally benign cement-like binders [10]. However, investigations deploying CDW in AAM formulations remain relatively sparse [11, 12, 13]. The existing research landscape predominantly explores AAM employing high levels of alkaline activators, with limited exploration of lower activator dosages. Consequently, holistic methodologies for recycling these waste residues remain elusive, with occasional inconclusive reports.

Effectuating efficient recycling mechanisms and the judicious application of chemicals to concrete waste could pave the way for a sustainable circular cement and concrete industry, addressing multifaceted environmental concerns [14]. Against the backdrop of extensive Portland cement usage in civil construction and the substantial CDW output, this study aims to assess the viability of integrating recycled concrete residue (RCR) into alkali-activated pastes. The investigation encompasses diverse levels of sodium hydroxide and sodium silicate additives, with subsequent curing at 100°C as a pivotal parameter for assessment.

The article is organized into four parts: 1 - introduction, with an overview of the topic; 2 - Materials and methods, with the description of the procedures to reach the objective; 3 - Results and discussions, with the main results obtained in the research and 4 - Conclusions.

II.   MATERIALS AND METHODS

The experimental design was directed to the execution of assays and analysis of data obtained from the characterizations of the RCR and the alkali-activated pastes. The methodology to be followed in this research consisted of four main stages: Preparation and characterization of the residue and preparation and characterization of the pastes.

2.1. Materials

The precursor used in this work is the RCR. The concrete waste to be recycled, comes from the work of adaptation of the sidewalks for external accessibility of the Morro do Cruzeiro Campus of the Federal University of Ouro Preto. This work was carried out in order to adapt the external area of the Campus to the locomotion of people with visual impairment and locomotive.

The concrete waste was collected in varying sizes, those with dimensions greater than 5 cm had their size reduced manually of a hammer and later all the residue was taken to a mill of manganese steel jaws. After passing through the jaw mill three times and reduced to a maximum diameter of 4.8 mm, this material was sieved for 5 minutes with the aid of the electric agitator and the material passing through the 0,6 mm sieve was defined as the precursor.

To define the RCR, the material went through a new grinding stage, in order to decrease the size of the grains and increase the specific area of the material. A study was carried out with grinding in a horizontal ball mill, with a speed of 50 rpm, in the time of 2 hours. Samples of all grinding times were collected to verify the granulometry.

To ensure better homogenization of the mixture, the powder activator sodium hydroxide (NaOH) was added during this grinding process. Another activator, sodium silicate (Na_2SiO_3), was used in liquid form and added along with the kneading water of the paste.

2.2. Mixes preparations

Prismatic specimens of dimensions 4x4x16 cm were produced in order to characterize the pastes and evaluate the viability of the alkaline activation of the RCR under study. The water/solids ratio was kept constant at 0,30. Traces were produced through simple alkaline activation with the addition of simple alkaline activator (Na_2SiO_3) and compound alkaline activation (NaOH and Na_2SiO_3).

The mixture of the paste was performed by means of a planetary mechanical mixer. The paste was mixed for a period of 3 minutes at low speed and then the molding of the specimens was performed. The molds with the pastes were then wrapped with plastic film and cured at room temperature (27 ℃)

for 24 hours and then in an oven at 100 ºC for 6 days. Table 1 presents the percentages of alkaline activators used, as well as the nomenclature of the specimens.

Table 1 – mixes of pastes.

Specimen	RCR (%)	Water (%)	NaOH (%)	Na₂SiO₃ (%)
H2S3	100	30	2	3
H2S9	100	30	2	9
H8S3	100	30	8	3
H8S9	100	30	8	9
H0S9	100	30	0	9

2.3. Paste characterization

The RCR sample was chemically characterized by the X-Ray Fluorescence (XRF) technique through the Epsilon 3x X-ray Spectrometer. The mineralogical analysis was performed by X-Ray Diffraction (XRD) equipment D2 PHASER 2nd Generation Bruker. The scanning electron microscope (SEM) assay in the equipment VEGA 3, TESCAN. The RCR laser diffraction particle size assay was performed from the Bettersize 2000 laser granulometer.

After the preparation of the specimens, they were characterized by the apparent density tests according to the recommendations of Brazilian standard NBR 13280 [15], scanning electron microscopy coupled to the energy dispersive X-ray detector (MEV / EDS), XRD equipment D2 PHASER 2nd Generation Bruker and compression strength test. The mechanical test of compressive strength was performed following the specifications of ABNT 13279 [16]. To determine the compressive strength, 6 prismatic specimens were used for each trait. For this test, an EMIC press model DL 20000 with a load cell of 20 kN was used. Data analysis of variance (ANOVA) was performed with the regression models tested by the F test and the means compared by the Tukey test. For the statistical analyses, the software Past - Paleontological Statistics [17] was used.

III.   RESULTS AND DISCUSSION

In the following items, the results obtained from the characterization of RCR and alkali-activated pastes are presented and discussed.

3.1. RCR Characterization

Through the XRF, it was possible to obtain the chemical composition of the RCR, as shown in Table 2. RCR is mainly composed of silicon oxides (SiO_2), calcium oxides (CaO) and magnesium oxides (MgO). It is observed that the residue under study has the two oxides that may be involved in the alkaline activation process: 42.2% silicon oxide (SiO_2) and a low amount of aluminum oxide (Al_2O_3): 6.09%. Calcium oxide makes up 31.3% of the RCR. Some studies [18, 19] found that calcium has a positive effect on the compressive strength of alkali-activated ligands. When the CaO content is high, the microstructural porosity decreases and the resulting formation of the amorphous structure increases the final mechanical strength [20, 21].

Table 2 – Chemical composition of RCR

Oxide	SiO_2	CaO	MgO	Al_2O_3	Fe_2O_3	Other
Mass (%)	42,2	35,3	7,7	6,1	5,4	3,2

Figure 1 shows the RCR diffractogram. The mineralogical analysis of the RCR shows that dolomite ($CaMg(CO_3)_2$), COD 36-0426, calcite ($CaCO_3$), COD 05-0586 and quartz (SiO_2), COD 46-1045, are the main minerals present in the RCR. Quartz and dolomite come from the aggregate present in the RCR. Yip et al. [22] report that the presence of dolomite and quartz particles act as a physical filler or microaggregate, aiding in compressive strength. Aggregates have a restrictive effect on shrinkage. Mastali [23] reports that aggregates can act on the alkali-activated pastes by decreasing the rate of retraction. It is suggested that the presence of calcite in the RCR is possibly due to the limestone filler

that makes up the anhydrous cement or the carbonation of calcium compounds in the cement matrix of the RC, such as portlandite $(Ca(OH)_2)$ or free lime (CaO).
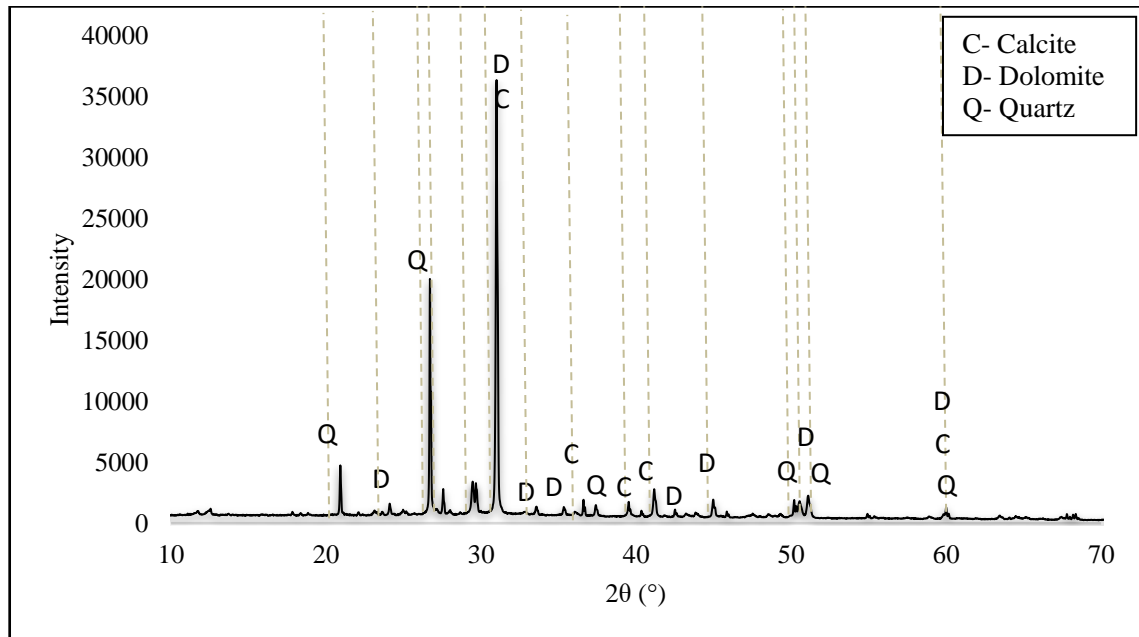

Figure 1 – RCR Diffractometry.

Laser particle size showed particles RCR with D90 of 116,3 μm and D50 of 13.,5 μm. Komnitsas et al. [24] reported the need for CDW-based particle size to be less than 150 μm and D50 less than 15 μm.

The micrographs of the concrete waste with magnification of 100x and 500x are presented in Figure 2. From the images obtained, it was possible to observe that the grains of residue are presented in varied sizes and shapes, and possibly the larger ground grains represent the fraction of aggregates and the smaller grains the cement paste.
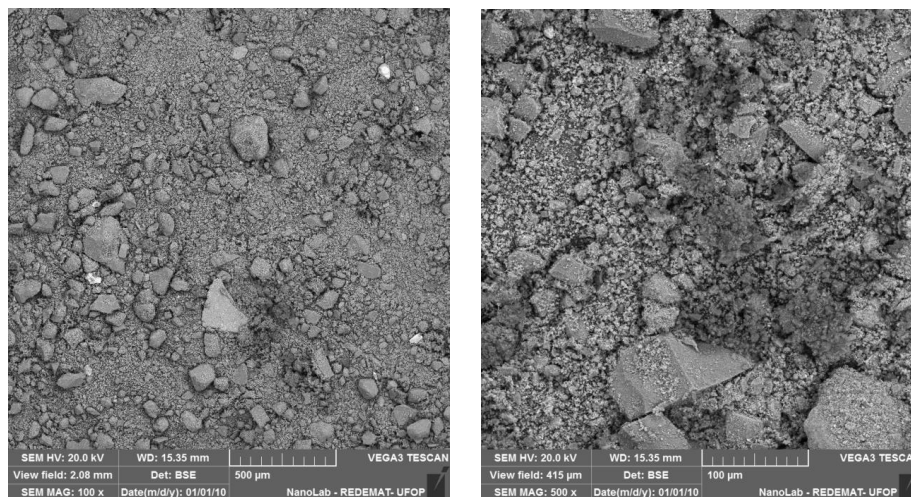

Figure 2 – SEM image of the concrete residue, with an increase of 100x and 500x respectively.

3.2. Paste Characterization

Figure 3 shows the compressive strength of the alkali-activated pastes at 7 days of curing. The compressive strength ranged from 2,12 MPa to 14,71 MPa. Note that the highest value of compressive strength was obtained for the paste that contains the highest percentage of NaOH and Na_2SiO_3. This corroborates with Palomo et al. [25] when reporting that the development of mechanical strength was

faster in samples activated with alkaline solutions combining hydroxides with soluble silicates. A highly alkaline environment favors the dissolution of aluminosilicate compounds by breaking Si–O–Si and Al–O–Al which, according to the polymeric model proposed by Davidovits [26], form a polymeric structure of aluminosilicate.
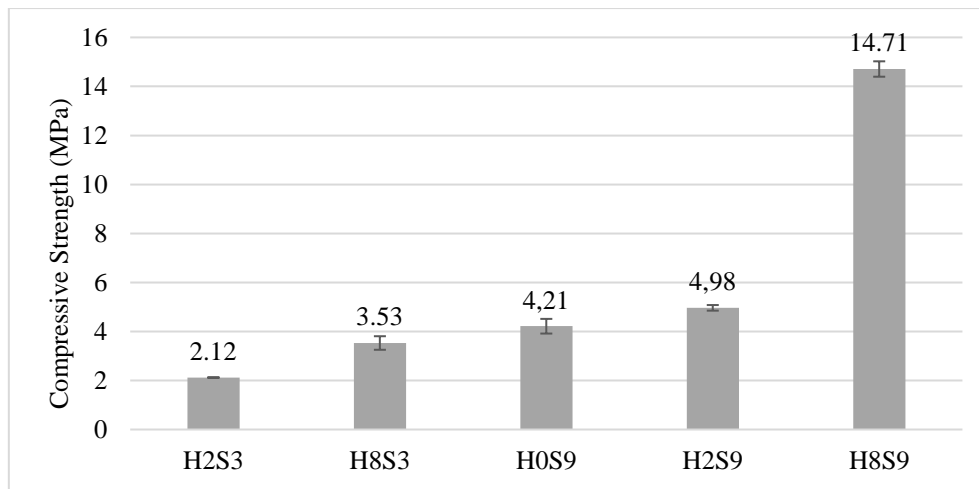

Figure 3 – compressive strength, seven days age.

Comparing the composite pastes with the same sodium hydroxide content (H2S3 x H2S9 and H8S3 x H8S9) and the pastes with the same sodium silicate content (H2S9 x H8S9 and H2S3 x H8S3), a resistance gain is observed as the activator content is increased. When comparing the pastes with 9 % silicate (H0S9, H2S9 and H8S9), which respectively present compressive strength of 4,21 MPa, 4,98 MPa and 14,71 MPa, there is an increase in the compressive strength in the composite pastes that used not only Na_2SiO_3 but also NaOH. With the increase in the concentration of NaOH, the dissolution of the raw materials is favored which consequently potentiates the alkali-activated reaction thus obtaining higher values of compressive strength. The NaOH solution is important for the dissolution of the Si and Al ions of the precursors, while the Na_2SiO_3 solution contains soluble silicate species and is therefore used to promote the condensation process in the alkali-activated reaction [27].

In the analysis of variance for compressive strength, the P-value lower than 0,05 and the F greater than the critical F reject the null hypothesis and verify a statistically significant difference between one or more groups as shown in Table 3.

Table 3 – ANOVA statistical analysis.

Source of variation	SQ	Gl	SQM	F	P-value	F critical
Between groups	435,53	4	108,88	242,90	1.94E-13	3,06
Within two groups	6,72	15	0,45			
Total	442,25	19				

In order to demonstrate which groups are statistically different from each other, the results of Tukey's method (Table 4) for compressive strength are presented, where the shaded cells indicate a statistically significant difference between the groups. Thus, according to Tukey's method all samples are statistically different from the H8S9 sample. The H2S3 sample besides being different from the H8S9 also differs from the H0S9 and H2S9 samples. For samples with 2 % NaOH content, the variation in Na2SiO3 content (9 % or 3 %) resulted in statistically different compressive strengths. Thus, when the Na2SiO3 content was fixed at 9 % (H0S9, H2S9 and H8S9), the addition of 0 % or 2 % of NaOH generated statistically equal resistances and only for the addition of 8 % of NaOH the compressive strength was statistically different. It is concluded that the variation in Na_2SiO_3 content seems to interfere more in the compressive strength than the variation in NaOH content.

Table 4 – Tukey's method.

Specimen	H2S3	H8S3	H0S9	H2S9	H8S9
H2S3		5,34E-02	3,12E-03	1,85E-04	0
H8S3	4,32		0,59	5,89E-02	1,02E-12
H0S9	6,41	2,091		0,5655	3,96E-12
H2S9	8,56	4,24	2,151		1,17E-11
H8S9	38,95	34,63	32,54	30,39	

3.2.1. Microstructural development

Figure 4 shows the result of the mineralogical analysis of the RCR and the pastes at 7 days of cure. For Fernández-Jiménez et al. [28] when the aluminosilicate source undergoes alkaline activation, the main component resulting from the reaction is an aluminosilicate gel with low order crystal structure.
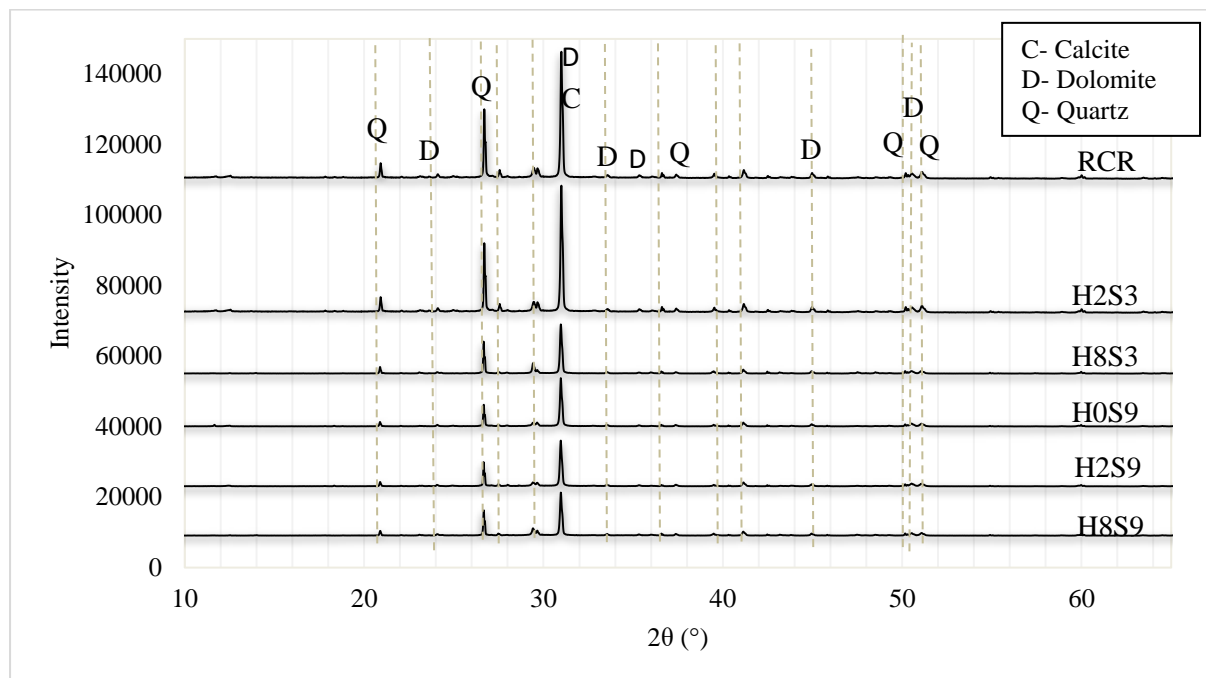

Figure 4 – Diffractogram of the RCR and the pastes with 7 days of cure.

When comparing the diffractograms of the source material with the diffractograms of the already hardened geopolymers, it is possible to observe that the crystalline phases remain, since there was no total dissolution of the crystals, however all the peaks appear in lower intensity. Lecomte et al. [29] report that although quartz remains in an inert phase, the high molarity could reduce its intensity due to the dilution effect. Vásquez et al. [30] report that in addition to dilution, a partial dissolution of certain crystalline phases may occur.

The pattern obtained shows a material with the same crystalline phases that were originally present in the RCR. This indicates that the changes responsible for the differences in compressive strength originate and occurred mainly within the amorphous part of the structure.

Figure 5 shows the micrograph of the H2S3 sample captured with magnification of 2000x and 5000x. It is observed that the material has a porous nature, with the presence of particles in various sizes and shapes, as well as unreacted particles that intertwine in small reacted clusters. The H2S3 sample presented the lowest result of compressive strength when compared to the other samples. Yunsheng et al. [31] report that weak particles that have not reacted can act as point defects, reducing the compressive strength of AAM. Insufficient alkaline activator is the main reason that leads particles not to react, since there is a delay in the initial dissolution of the compounds [32].
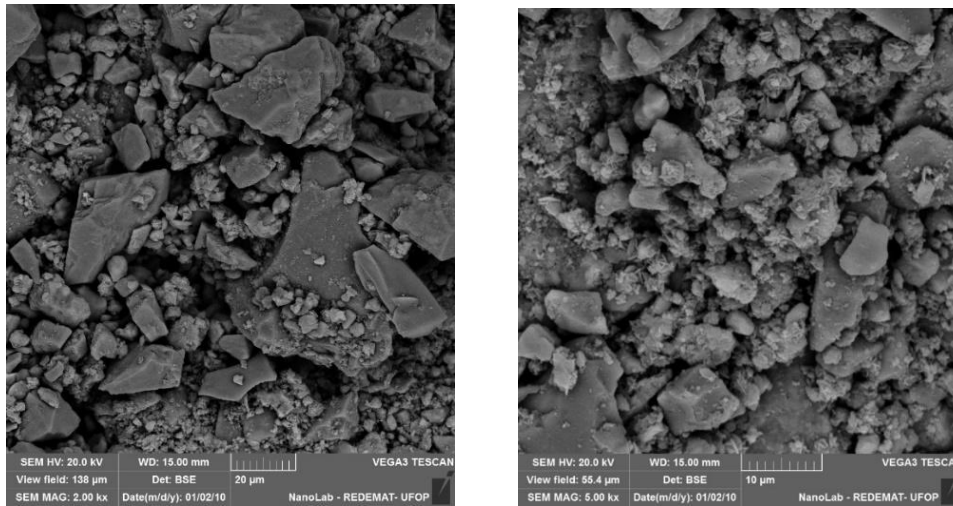
Figure 5 - Micrograph of the H2S3 sample, 2000x and 5000x magnification.

In Figure 6, the micrograph of the H8S3 sample is presented, captured with magnification of 2000x and 5000x, the paste is characterized by having a denser and homogeneous matrix which goes against when compared to the H2S3 sample.
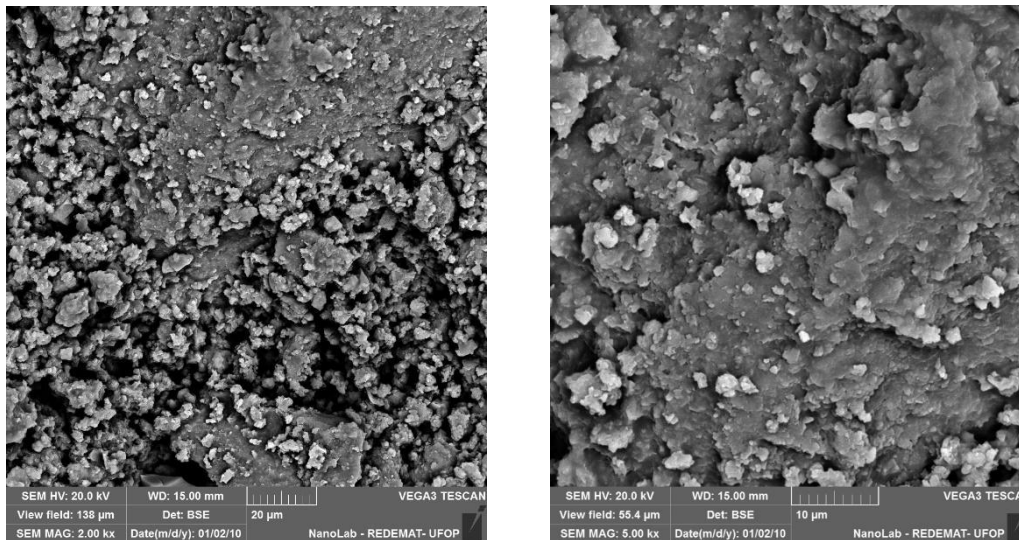

Figure 6 - Micrograph of the sample H8S3,2000x and 5000x.

Figure 7 shows the micrograph of the sample H0S9 captured with magnification of 2000x and 5000x. The paste is characterized by having a porous structure with dispersed and unreacted particles as a consequence of the use of only one alkaline activator, Na_2SiO_3. Simple activators result in a less reactive and seemingly incomplete process when compared to compound activators. Alkaline hydroxide has the function of dissolving raw materials, while alkaline silicate solution acts as a binder [33].

Associated with the SEM analysis, the point chemical analysis by EDS (X-ray dispersive energy) of the energy of the backscattered electrons (BSE) of the samples H2S9 and H8S9 was used, with magnification of 2000x.

Figure 8 shows the point chemical analysis of the H2S9 sample captured with 2000x magnification, where Figure 8 (a) shows the demarcation of the areas selected for point chemical analysis and Figure 8 (b) shows the mapping of the distribution of chemical elements in the sample. The semi-quantitative results are shown in Table 5. It is suggested that point 1 is unreacted quartz since the point analysis showed a majority constitution of silicon. The presence of an incomplete reaction is confirmed by the low content of silicon and sodium in the interfaces of the matrix, represented by point 2 and are presented on the micrograph in greenish tone, evidencing the presence of calcium. Point 3 has a Ca/Si ratio of 1.3 and Si/Al ratio of 3.2, suggesting that they are CASH gels.
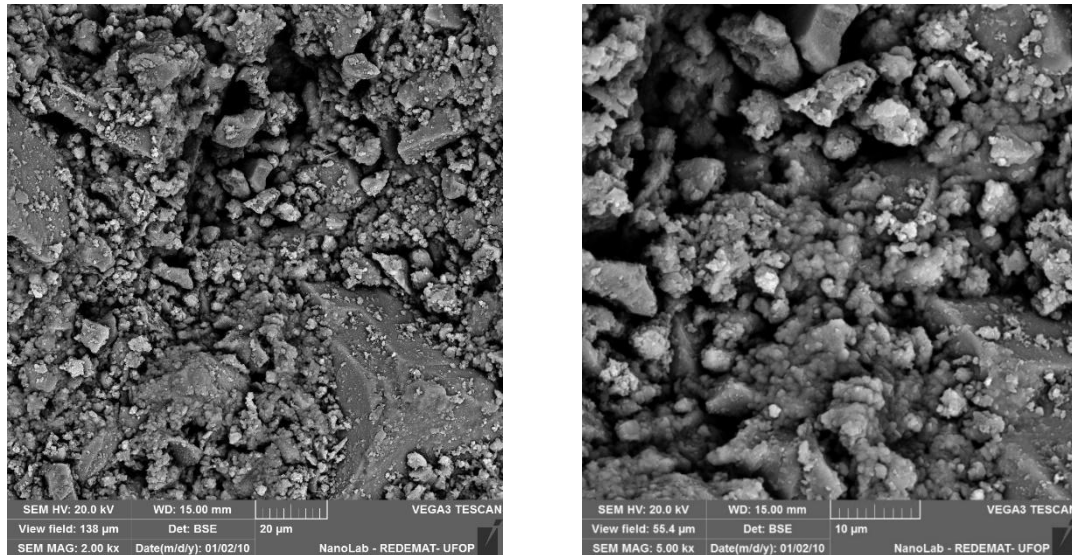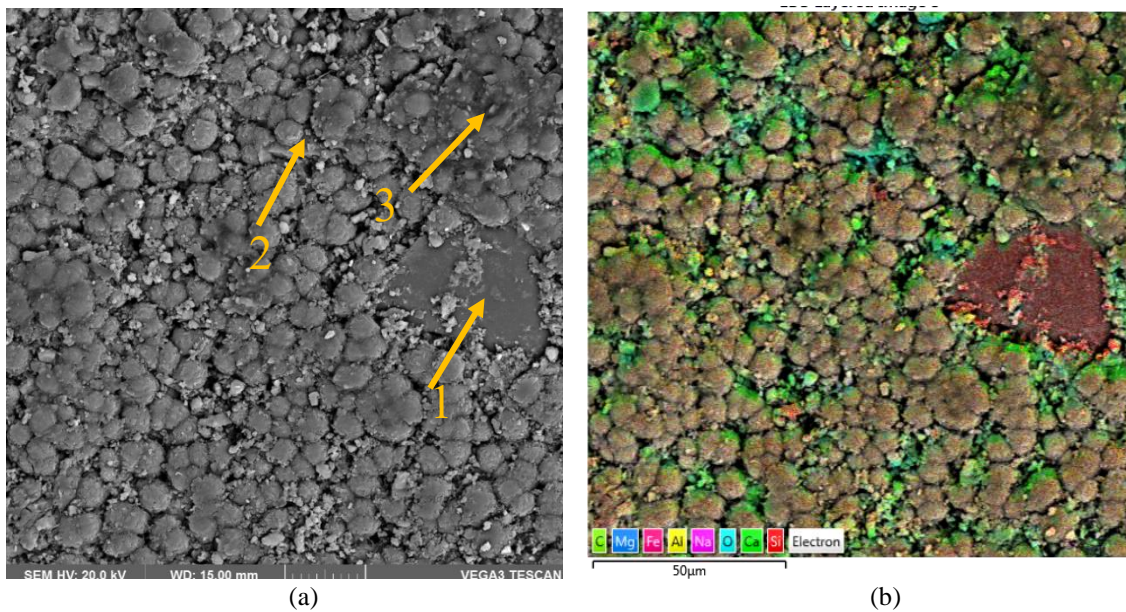
Figure 7 - Micrograph of sample H0S9, 2000x and 5000x.

(a)   (b)
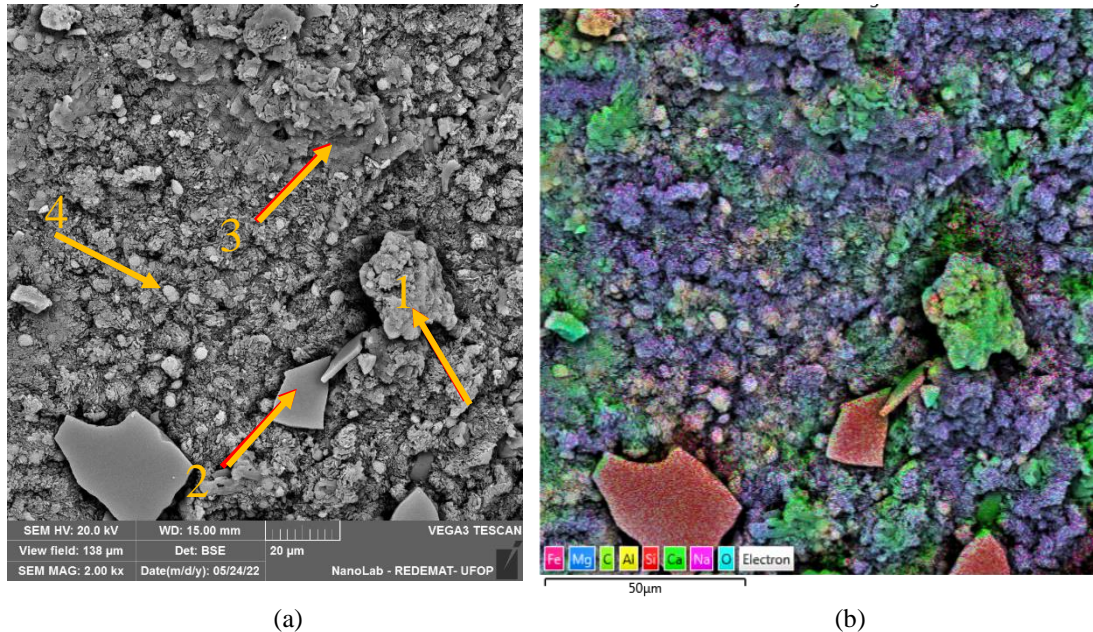
Figure 8 - Micrograph of sample H2S9, 2000x.

Table 6 - Semiquantitative chemical analysis of the H2S9 sample.

Element	Points		
(%)	**1**	**2**	**3**
Si	38,7	3,0	17,0
Al	-	1,6	14,2
Ca	0,4	19,0	1,2
Mn	-	1,3	-
Mg	-	9,6	-
Fe	0,2	2,4	0,4
Na	0,7	1,9	4,1
C	7,9	9,5	18,4
O	52,1	51,8	43,3

Figure 9 shows the point chemical analysis of the H8S9 sample captured with 2000x magnification, where Figure 9 (a) presents the demarcation of the areas selected for point chemical analysis and Figure 9 (b) shows the mapping of the distribution of chemical elements in the sample.

The semiquantitative results of the chemical analysis of the H8S9 sample are shown in Table 7. In the punctual chemical analysis it was observed that Point 1 is basically composed of calcium, with low

contents of silicon and sodium, suggesting that it is the product of efflorescence. The main products of efflorescence are sodium carbonates in hydrated or anhydrous forms, which grow in different shapes and sizes [34]. It is suggested that Point 2 is unreacted quartz since the point analysis showed a majority of silicon. Point 3 has a Ca/Si ratio of 2.1 and Si/Al of 1.8, suggesting that they are CASH gels. Provis and Bernal [35] associated the formation of C-A-S-H gel with the presence of reaction secondary products in systems rich in aluminum and/or magnesium. A more homogeneous and less porous matrix is observed around Point 3. Note the presence of whitish spherical points distributed by the matrix, as pointed out by Point 4. Point 4 consists of a large amount of sodium suggesting that it is unreacted NaOH.

(a)   (b)

Figure 9 - Micrograph of sample H8S9, 2000x.

Table 7 - Semiquantitative chemical analysis of the H8S9 sample.

Elements	Points			
(%)	1	2	3	4
Si	6,2	40,6	4,4	2,6
Al	1,2	-	2,4	2,2
Ca	33,9	1,6	9,4	12,7
Mg	-	-	1,4	-
Fe	5,2	-	1,1	0,4
Na	4,0	6,5	27,2	29,7
C	2,9	-	9,8	4,6
O	35,1	51,3	44,4	47,9

IV.   CONCLUSIONS

The assessment procedures revealed the viability of utilizing RCR for the synthesis of alkali-activated material through both composite activation involving NaOH powder and sodium silicate solution, as well as for singular activation employing Na2SiO3 solution. The paramount compressive strength outcome was observed in the context of composite alkaline activation, registering a peak value of 14.7 MPa after 7 days of curing, utilizing an 8% NaOH concentration and a 9% Na2SiO3 concentration. It is conjectured that enhanced control over efflorescence could yield even higher compressive strength outcomes. A scrutiny of variance highlighted that deviations in sodium silicate composition exert more pronounced influence on mechanical strength compared to fluctuations in sodium hydroxide content.

ACKNOWLEDGEMENTS

REFERENCES

[1]. Torgal, F. P. & Jalali, S. (2010) A *Sustentabilidade dos Materiais de Construção.* Publindústria, Available at: https://hdl.handle.net/1822/28852. In portuguese.

[2]. Villaquirán-Caicedo, Mónica A. & de Gutiérrez, Ruby Mejía. "Comparison of different activators for alkaline activation of construction and demolition wastes." *Construction and Building Materials*, v. 281, pp. 122599, 2021.

[3]. Robayo-Salazar, Rafael; Valência-Saavedra, William & De Gutiérrez, Ruby Mejía. (2022) "Recycling of concrete, ceramic and masonry waste via alkaline activation: Obtaining and characterizing hybrid cements". *Journal of Building Engineering*, v. 46, p. 103698.

[4]. Abrelpe – Brazilian Association of Public Cleaning and Special Waste Companies. *Panorama dos resíduos sólidos 2020*. São Paulo: Abrelpe, 2021. In portuguese.

[5]. Melo, Estela Violin et al. (2021). "Construction and demolition waste: a review of uses and applicability on roads and highways (2015 – 2020)". *Research, Society and Development*, v. 10, n. 10, p. e286101018658.

[6]. Bessa, Sofia Araújo Lima; Gonçalves, Tiago Augusto & Lourenço, Karen Katleen (2019)." Análise quantitativa e qualitativa dos resíduos de construção e demolição gerados em Belo Horizonte/MG.". *Revista Brasileira de Gestão Urbana*, v. 11, 2019. In portuguese.

[7]. Shi, Caijun; Jiménez, A. Fernández & Palomo, Angel. (2011) "New cements for the 21st century: The pursuit of an alternative to Portland cement." *Cement and concrete research*, v. 41, n. 7, pp. 750-763.

[8]. Provis, John L. "Alkali-activated materials." *Cement and Concrete Research*, v. 114, p. 40-48, 2018.

[9]. Severo, C. G. S. et al. (2013) "Características, particularidades e princípios científicos dos materiais ativados alcalinamente." *Revista eletrônica de Materiais e Processos*, v. 8, n. 2, p. 55-67. In portuguese.

[10]. Provis, John L. et al (2009). "High-resolution nanoprobe X-ray fluorescence characterization of heterogeneous calcium and heavy metal distributions in alkali-activated fly ash." *Langmuir*, v. 25, n. 19, pp. 11897-11904.

[11]. Das, Sourav Kumar & Shrivastava, Sandeep (2021). "Influence of molarity and alkali mixture ratio on ambient temperature cured waste cement concrete based geopolymer mortar." *Construction and Building Materials*, v. 301, p. 124380.

[12]. Abdel-Gawwad, Hamdy A.; Rashad, Alaa M. & Heikal, Mohamed (2019). "Sustainable utilization of pretreated concrete waste in the production of one-part alkali-activated cement." *Journal of Cleaner Production*, v. 232, pp. 318-328, 2019.

[13]. Lampris, C.; Lupo, R. & Cheeseman, Christopher R. (2005). "Geopolymerisation of silt generated from construction and demolition waste washing plants." *Waste Management*, v. 29, n. 1, p. 368-373.

[14]. Ho, Hsing-Jung; Iizuka, Atsushi & Shibata, Etsuro (2021). "Chemical recycling and use of various types of concrete waste: A review." *Journal of Cleaner Production*, v. 284, p. 124785.

[15]. ABNT – Brazilian Association of Technical Standards (2005). *NBR 13280 – Argamassa para assentamento e revestimento de paredes e tetos - Determinação da densidade de massa aparente no estado endurecido.* ABNT, Rio de Janeiro. In Portuguese.

[16]. ABNT – Brazilian Association of Technical Standards (2005). *NBR 13279 – Argamassa para assentamento e revestimento de paredes e tetos - Determinação da resistência à tração na flexão e à compressão.* ABNT , Rio de Janeiro. In Portuguese.

[17]. Hammer, Ø.; Harper, D. A. T. & Ryan, P. D. *PAST: Paleontological Statistics Software Package*, 2001.

[18]. Xu, Hua & Van Deventer, J. S. J. (2000). "The geopolymerisation of alumino-silicate minerals." *International Journal of Mineral Processing*, v. 59, n. 3, pp. 247-266.

[19]. Yip, C. K.; Lukey, G. C. & Van Deventer, J. (2005). "The coexistence of geopolymeric gel and calcium silicate hydrate at the early stage of alkaline activation." *Cement and concrete research*, v. 35, n. 9, p. 1688-1697.

[20]. Van Jaarsveld, J. G. S.; Van Deventer, J. S. J. & Lorenzen, L. L. (1998). "Factors affecting the immobilization of metals in geopolymerized fly ash." *Metallurgical and materials transactions B*, v. 29, n. 1, pp. 283-291.

[21]. Xu, Hua & Van Deventer, Jannie (2002). "Microstructural characterisation of geopolymers synthesised from kaolinite/stilbite mixtures using XRD, MAS-NMR, SEM/EDX, TEM/EDX, and HREM." *Cement and Concrete Research*, v. 32, n. 11, pp. 1705-1716.

[22]. Yip, Christina K. et al. (2008) "Carbonate mineral addition to metakaolin-based geopolymers." *Cement and Concrete Composites*, v. 30, n. 10, pp. 979-985.

[23]. Mastali, M. et al. (2018). "Drying shrinkage in alkali-activated binders – a critical review". *Construction and Building Materials*, v. 190, pp. 533-550.

[24]. Komnitsas, Kostas et al. (2015) "Effect of synthesis parameters on the quality of construction and demolition wastes (CDW) geopolymers." *Advanced Powder Technology*, v. 26, n. 2, pp. 368-376.

[25]. Palomo, A. et al. (1999). "Chemical stability of cementitious materials based on metakaolin." *Cement and Concrete Research*, v. 29, n. 7, pp. 997-1004.

[26]. Davidovits, Joseph (1982). "Mineral polymers and methods of making them." U.S. Patent n. 4.349.386. 14 sep. 1982.

[27]. Panias, Dimitrios; Giannopoulou, Ioanna P. & Perraki, Theodora (2007). "Effect of synthesis parameters on the mechanical properties of fly ash-based geopolymers." *Colloids and Surfaces A: Physicochemical and Engineering Aspects*, v. 301, n. 1-3, pp. 246-254.

[28]. Fernández-Jiménez, Ana & Palomo, A. (2005). "Mid-infrared spectroscopic studies of alkali-activated fly ash structure." *Microporous and mesoporous materials*, v. 86, n. 1-3, pp. 207-214.

[29]. Lecomte, I., Liégeois, M., Rulmont, A., Cloots, R., & Maseri, F. (2003). "Synthesis and characterization of new inorganic polymeric composites based on kaolin or white clay and on ground-granulated blast furnace slag." *Journal of Materials Research*, 18(11), pp. 2571-2579.

[30]. Vásquez, A., Cárdenas, V., Robayo, R. A., & de Gutiérrez, R. M. (2016). "Geopolymer based on concrete demolition waste." *Advanced Powder Technology*, 27(4), pp. 1173-1179.

[31]. Yunsheng, Zhang et al (2007). "Synthesis and heavy metal immobilization behaviors of slag based geopolymer." *Journal of Hazardous Materials*, v. 143, n. 1-2, pp. 206-213.

[32]. Trochez, J. J. et al (2015). "Synthesis of geopolymer from spent FCC: Effect of SiO_2/Al_2O_3 and Na_2O/SiO_2 molar ratios." *Materiales de Construcción*, v. 65, n. 317, p. e046.

[33]. Cheng, Ta-Wui & Chiu, J. P (2003). "Fire-resistant geopolymer produced by granulated blast furnace slag." *Minerals engineering*, v. 16, n. 3, pp. 205-210.

[34]. Yao, Xiao; Yang, Tao; Zhang, Zuhua (2016). "Compressive strength development and shrinkage of alkali-activated fly ash–slag blends associated with efflorescence." *Materials and Structures*, v. 49, n. 7, pp. 2907-2918.

[35]. Provis, John L. & Bernal, Susan A (2014). "Geopolymers and related alkali-activated materials." *Annual Review of Materials Research*, v. 44, pp. 299-327.

Authors

Edna Paula da Costa Reis holds a degree in Civil Engineering from the Federal University of São João del Rei (UFSJ) and a Master's Degree in Construction Engineering in the area of construction materials (MECON – UFOP), with emphasis on the study and development of alkali-activated materials. Currently, she works as a technician at the Department of Projects of the Federal University of Ouro Preto.

https://orcid.org/0000-0001-6327-0313

Guilherme Jorge Brigolini Silva holds a degree in Civil Engineering from the Federal University of Minas Gerais (1999), a PhD in Materials Science from the Postgraduate Course in Metallurgical and Mining Engineering of the Federal University of Minas Gerais (2011). He is currently an Associate Professor with exclusive dedication at the Federal University of Ouro Preto and a professor in the Graduate Program PROPEC and MECOM. Coordinator of the Research Group ATIVE - CNPq.

https://orcid.org/0000-0001-8444-9451

Jose Carlos Borba Jr holds a degree in Civil Engineering from the Federal University of Paraiba (2006), a master degree in Civil construction at Federal University of Espirito Santo (2011). He is currently an Adjunct Professor with exclusive dedication at the Federal University of São João Del-Rei.

https://orcid.org/0000-0002-2224-583X